PAPER

Check for updates

Synthesis and characterization of silica gel from Lapindo volcanic mud with ethanol as a cosolvent for desiccant applications

Qurrota A'yuni, [ID] *[abf] Ardhana Rahmayanti,[c] Hartati Hartati,[a] Purkan Purkan,[a] Riki Subagyo,[d] Nihayatur Rohmah,[e] Luthfiyah Rifdah Itsnaini[a] and Medya Ayunda Fitri [ID] [b]

Lapindo mud (LM) is a volcanic mud from a natural disaster that occurred 16 years ago in Sidoarjo District, East Java, Indonesia. The high amount of silica in the local materials of LM has been extracted for silica gel synthesis *via* hydrometallurgy methods, followed by sol–gel methods. The presence of ethanol in the synthesis process generated a unique textural property at different ratios between ethanol and sodium silicate (e/ss). Sol–gel mediated silica gel synthesis exhibited mesoporous properties with an amorphous structure, which is a characteristic of the silica gel. The silica gel exhibits silica nanoparticles over the average diameter of 2.08 nm with a spherical morphology and is connected to form an agglomeration structure. Increasing the e/ss ratio enhanced the amount of the hydroxyl group and the specific surface area ranged from 57 to 103 $m^2 g^{-1}$. The moisture adsorption performance of each silica gel showed that the silica gel with an e/ss ratio of 5 : 5 exhibited the highest adsorption capacity measured by conventional gravimetric methods and thermogravimetric analysis of 10.56% and 11.20% $g_{water} g_{silica}^{-1}$, respectively. These results indicated that the silica gel with an e/ss ratio has a high number of hydroxyl groups and more surface-active sites, which is beneficial for the adsorption process. The adsorption capacity of the synthesized silica gel is also higher than that of the commercial silica gel, indicating an excellent performance for desiccant applications.

Introduction

Desiccant is a material needed to minimize the presence of water in air. The presence of moisture in air causes mold growth and damages electronic devices prone to corrosion. Thus, air humidity regulation is very important to avoid its effect. Therefore, adding desiccant to some electronic devices, food storage, and other industrial applications is essential to reduce humidity.[1,2] Silica gel is a desiccant that is usually used in laboratories or storage. Commonly, commercial silica gel has various colors, including blue, transparent, and brown, and is in the form of crystal-like spheres. Especially for blue silica gel,

the color would change into pink due to the adsorption of humidity on its surface.[3] The silica gel is an amorphous form of silica that has significant use due to the water adsorption ability.[4] The high ability of water adsorption is because of porosity and Si–O–H groups of the silica gel structure. Commonly, the silica gel is fabricated from the acidification process of sodium silicate.[5] The synthesis of sodium silicate needs a high amount of energy to break the strong bonds of Si–O.[6] For instance, sodium silicate is synthesized by a high-temperature treatment (1300–1500 °C) of quartz and sodium carbonate.[7,8]

To minimize the cost of production, researchers have developed the synthesis of silica using natural sources due to its low cost and high availability. One natural source that can be utilized for the silica gel synthesis is Lapindo mud (LM). LM is a volcanic mud from a natural disaster that occurred 16 years ago in Sidoarjo District, East Java, Indonesia,[9] whose cause is unclear to date.[10,11] LM contains a high concentration of silica, making it very suitable for silica synthesis.[4,12] Using LM in silica fabrication also increases value-added properties of LM and minimizes the utilization of laboratory-grade reagents. Moreover, LM also contains some compounds such as alumina (Al_2O_3), iron oxide (Fe_2O_3), calcium oxide (CaO), strontium oxide (SrO), and manganese(II) oxide (MnO), which need to be

[a]Department of Chemistry, Faculty of Science and Technology, Universitas Airlangga, Surabaya 60115, Indonesia. E-mail: qrayuni@gmail.com

[b]Department of Chemical Engineering, Faaculty of Engineering, Universitas Nahdlatul Ulama Sidoarjo, Sidoarjo 61234, Indonesia

[c]Department of Environmental Engineering, Faculty of Engineering, Universitas Nahdlatul Ulama Sidoarjo, Sidoarjo 61234, Indonesia

[d]Department of Chemistry, Faculty of Science and Data Analytics, Institut Teknologi Sepuluh Nopember, Surabaya 60111, Indonesia

[e]Department of Wood & Paper Science, Kyungpook National University, Daegu 41566, South Korea

[f]Supra Modification and Nano-Micro Engineering Research Group, Universitas Airlangga, Surabaya 60115, Indonesia

separated to obtain high purity silica *via* thermal treatment or acid treatment. However, these methods separate silica imperfectly and need to be improved to obtain high purity silica.

Silica was fabricated from bentonite by combining thermal treatment and acid treatment.[13] This process is better for separating silica from natural sources than one-step separation methods. In addition, this process can also control the particle size by adding cosolvents such as alcohols (ethanol or methanol) or other organic solvents miscible with water. The cosolvent influences the formation of alkoxide compounds in the pore, which is then removed *via* the last heat treatment.[14] The presence of cosolvent also reduces the particle size of silica, providing a large specific surface area that is a crucial factor for the adsorption process.

Following the observation, we fabricated the silica from Lapindo volcanic mud, which is a local material obtained from natural disasters in Sidoarjo Indonesia by combining acid and thermal treatment with various compositions of cosolvent (mixing of ethanol–water) to control the pore size and surface area. Ethanol was chosen as a cosolvent due to its good miscibility with silica solution, promoting the polycondensation process and controlling their textural properties.[14,15] Combining thermal and acid treatment can reduce the side compound (*e.g.*, Fe_2O_3, CaO, SrO, and MnO) and enhance the concentration of silica. The obtained silica was applied in desiccant *via* conventional gravimetric measurement and thermal gravimetric analysis (TGA). For comparison, commercial silica was also used for desiccant applications by conventional gravimetric measurement. Finally, the correlation between the influence of adding ethanol as a cosolvent to the silica gel properties and its resulting in the adsorption process is also discussed to make a clear statement of this modification.

Methodology

Materials

LM was taken from Sidoarjo, East Java, Indonesia about 1 km from the mudflow center and taken on the surface of mud land to a depth of 50 meters. All chemicals for the preparation and synthesis of silica gel, namely, hydrochloric acid (HCl, 37%), sodium hydroxide (NaOH, 99%), ethanol absolute (EtOH, 99.9%), and silver nitrate (AgNO_3, 99.8%) were purchased from Merck, Germany.

LM treatment

LM was left at 120 °C for 24 hours to remove the moisture content. The dried LM were crushed and sifted into 140 mesh sieves to obtain the uniform particle size of ±105 μm. LM was leached by adding 5 M HCl with a ratio of 1 : 5 (w/v). The mixture was stirred for 2 hours at 60 °C. The obtained solids were neutralized by adding distilled water. The mixture was left for a night. The mixture generated the yellowish filtrates, which was then separated by the decantation process to remove the filtrates. This process was repeated several times until the transparent filtrates were obtained. The solid was dried for 24 hours at 100 °C to remove the water content. The leached solid

was labeled as LLM. Furthermore, LLM was calcined at 680 °C for 1 hour and labeled as TLM.

Silica gel synthesis

The silica gel was synthesized by the sol–gel method. Firstly, 20 g TLM were mixed with 200 mL 2 M NaOH. The mixture was refluxed for 2 hours at 90 °C. The results were filtered to separate sodium silicate solution. EtOH as a cosolvent was added to the sodium silicate solution. The volume ratio of ethanol and sodium silicate (e/ss) were varied as 1 : 5, 2 : 5, 3 : 5, 4 : 5, and 5 : 5. The mixture was heated at 50 °C under stirring constant. The mixture was neutralized using 5 M HCl and the temperature was maintained at 50 °C. The mixture was aged for 18 hours at room temperature. The obtained gel was washed with distilled water to remove the impurities. AgNO_3 was used to test the presence of any Cl^- within the waste filtrate. The gel was dried at 80 °C for 18 h until the weight of the gel was constant. The average yield of the obtained silica gel was 2.78 g (~14%).

Characterization

Lapindo mud composition was analyzed using X-ray fluorescence spectrophotometer (XRF, PANalytical MiniPal 4) at 30 kV. X-Ray diffraction (XRD, PANalytical X'Pert MPD No. 1) was used to characterize the structure and phase of Lapindo mud and silica gel. The functional group of Lapindo mud and silica gel were identified using Fourier transform infrared (FTIR, Shimadzu IR Tracer-100) spectroscopy *via* KBr methods in the wavenumber range of 4000–400 cm^{-1}. The surface morphology of silica gel was characterized using scanning electron microscopy (SEM), which was fulfilled with energy dispersive X-ray (EDX) spectrophotometry to determine the composition of silica gel. The surface area and pore distribution of silica gel were analyzed using the N_2 adsorption–desorption technique observed by Quantachrome Quadrasorb-Evo. The thermal stability of the silica gel was analyzed by thermogravimetric analysis (TGA, Mettler Toledo).

Water vapor adsorption test

The adsorption test was carried out by the gravimetric method. Silica gel was heated at 120 °C for 1 hour. Then, the silica gel was stored in the desiccator, which was filled with water. The relative humidity (RH) varied by 70%, 80%, and 90% at a constant temperature of 29 ± 1 °C was measured by a calibrated hygrometer. Silica was weighed every 30 minutes for 3 hours to determine the weight change. The adsorption capacity was calculated using eqn (1) as follows.

$$\text{Adsorption ability } (\%) = \frac{\text{mass of adsorbed water}}{\text{mass of silica}} \times 100\% \quad (1)$$

The adsorption capability of silica gel toward water was also determined by the TGA technique by identifying the weight loss of silica gel. In TGA technique, a temperature of 100 °C was chosen as the boiling point of water to study the thermal events of water evaporation to determine the adsorption capacity of silica gel and the suitability of the results with conventional

adsorption tests. The adsorption ability of the obtained silica gel was calculated as follows.

$$\text{Adsorption ability (\%)} = \frac{\text{mass of silica lost at } 100\ ^\circ C}{\text{mass of initial silica}} \times 100\%$$

(2)

Results and discussion

Characterization

LM, LLM, and TLM were characterized by XRD to determine the composition of each component. The elemental compositions of LM, LLM, and TLM are summarized in Table 1. Before the treatment process, Fe_2O_3 concentration in LM is higher, which might can interfere with the silica gel synthesis. However, the silica concentration in LLM is the highest composition, indicating that LM can be used for silica gel synthesis. Followed by acid leaching treatment, the concentration of Fe_2O_3 reduces due to the ionization process of Fe to Fe^{3+} during the addition of HCl.[16,17] In addition, other compounds in LM are also reduced after the acid leaching treatment, while the silica composition is increased. The concentration of Fe_2O_3 is decreased after the heating treatment and resulted in increasing silica content about ~15%. The thermal treatment can enhance the mud reactivity in the extraction process, indicated by increasing silica purity.[13]

Next, we have characterized using XRD to investigate the crystallinity structure and phase transition of LM, LLM, TLM, and silica gel (e/ss of 5 : 5). According to the diffractogram in Fig. 1, LM exhibits a diffraction peak of SiO_2 at $2\theta = 26.55°$, which is confirmed by JCPDF no. 00-006-0221.[18] The sharp peak of SiO_2 reveals that SiO_2 in LM has high crystallinity. In addition, some peaks are observed at $2\theta = 34.89°$, $30–40°$, and $50.06°$. These peaks are attributed to the CaO,[19,20] Al_2O_3,[21] and Fe_2O_3 (ref. 22) peaks and correspond to the JCPDS no. 01-082-1691, 86-1410, and 39-1346, respectively. After the leaching process, the intensity of crystalline SiO_2 diffraction peak is increased due to the increasing purity of SiO_2. However, the diffraction pattern of the synthesized silica gel shows a broad intensity peak of SiO_2 only by the absence of any diffraction peak of the crystalline structure. The broad peak confirms the formation of amorphous silica phase and reveals the hexagonal symmetry of quartz silica. This result is similar to the diffraction
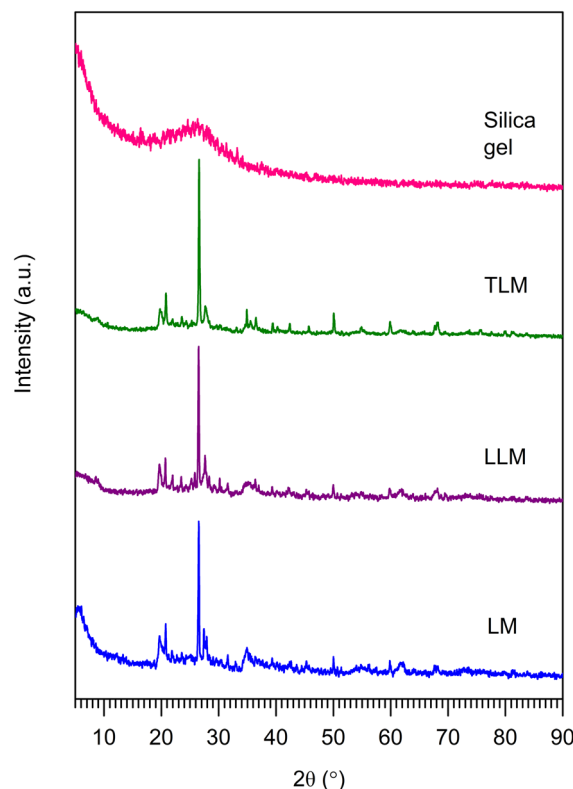

Fig. 1 XRD pattern of the prepared Lapindo volcanic mud and synthesized silica gel.

pattern of silica synthesized from corn.[23] Moreover, the XRD pattern suggests the effectiveness of our proposed method for the production of silica gel.

To identify the functional groups in silica gel, FTIR analysis was carried out *via* KBr methods. The FTIR spectra of silica gel is shown in Fig. 2. All samples exhibit the Si–O–Si longitudinal stretching vibration band at 1220 cm^{-1}, while the absorption band at 1060 cm^{-1} is attributed to the transverse stretching vibration of Si–O–Si.[24] The external symmetric stretching vibration of Si–O–Si is observed at 798 cm^{-1}.[25] The symmetric stretching vibration of Si–OH is observed at 960 cm^{-1}.[26] The absorption band at 1640 cm^{-1} is associated to the –OH absorbed on the silica gel surface, which is supported with the board peak at 3600–3400 cm^{-1}.[27] Increasing the volume of ethanol led to an increase in the intensity of the Si–O–H vibration at 960 cm^{-1}, demonstrating that the presence of ethanol promotes the hydrolysis process in the reaction. Compared with the IR spectra of LM, the intensity of absorption band at 960 cm^{-1} of the synthesized silica gel is broader, revealing the formation of the amorphous silica phase. This result was in agreement with the XRD results.

Adsorption–desorption N_2 was carried out to determine the textural properties of silica gel. The adsorption–desorption N_2 behavior and pore diameter distribution of silica gel with various ratio of e/ss is shown in Fig. 3. All samples exhibit the type IV isotherm based on the IUPAC classification, indicating the characteristic of mesoporous materials.[28] Increasing the e/ss

Table 1 Compound composition of LM, LLM, and TLM by XRF analysis

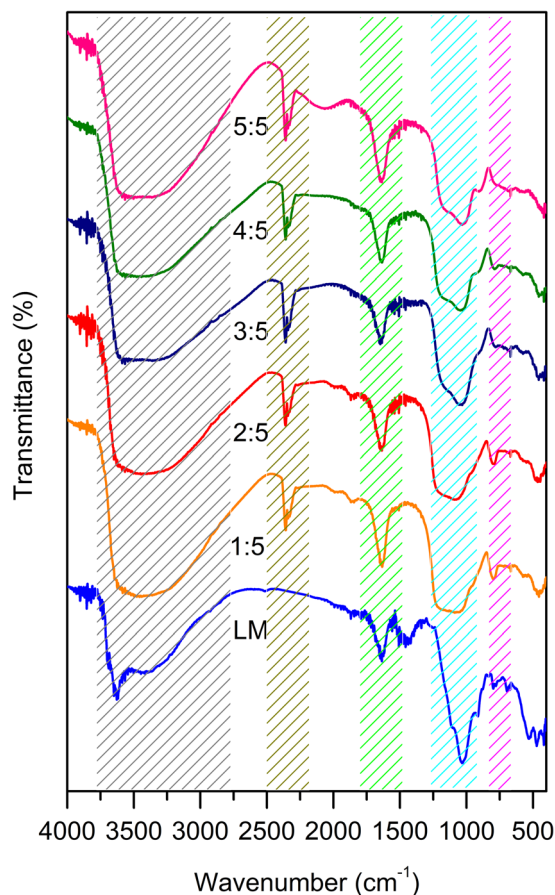| Compound	Concentration (%)		
	LM	LLM	TLM
SiO_2	49	62	64
Fe_2O_3	27.4	12.7	11.9
Al_2O_3	14	14	14
CaO	8.5	2.7	2.9
SrO	0.49	0.08	0.08
MnO	0.44	0.07	0.07
CuO	0.14	0.11	0.11
ZrO_2	0.1	0.1	0.09
V_2O_5	0.1	0.08	0.06
Rb_2O	0.04	0.04	0.03

Fig. 2 FTIR spectra of the silica gel at various e/ss ratio.

ratio, the hysteresis loop is generated due to the capillary condensation. The hysteresis loop shows type III (H3), whose adsorption profile demonstrated that the size is non-uniform

for this mesoporous material with slit-shaped pores.[29] The H3 type also reveals that the nitrogen condensation occurred between the interparticle voids that formed due to the textural porosity between the particles.

Fig. 3b shows the pore size distribution of silica gel at various e/ss ratio, as derived using BJH methods. The pore size at the e/ss ratio of 1 : 1 is slightly different compared to the e/ss ratio of 2 : 1 and 3 : 1. Increasing the e/ss ratio of 4 : 1, the pore size is enhanced and reduced at e/ss ration of 5 : 1 with a fairly uniform distribution. According to Table 2, the surface area of the silica gel increases along with increasing e/ss ratio from 2 : 5 to 5 : 5; likewise, for the pore volume and average pore diameter. The presence of ethanol in the solvent promotes the poly-condensation process during the sol–gel process, acting as a template-like on the pore of gel to form more hollow pores in the silica gel after heat treatment. Heating the gel can cause the gel pores to become vacant due to the release of alkoxide molecules that originally filled the gel pores. Compared to the LM (Fig. 3c), the pore size of the obtained silica gel is decreased but the pore volume is increased, attributed to the pore formation during the polycondensation process.

The SEM-EDX of silica gel (5 : 5) is displayed in Fig. 4. Silica gel exhibits aggregated particles with spherical morphology connected with each other. The determination of silica particles is carried out using ImageJ and exhibits the particle size of the silica gel as $2.08333 \pm 0{,}00514$ nm with a deviation standard of 0.99091. It can be seen that silica gel is a nanoparticle. The EDX analysis of silica gel shows that silica gel contains silicon (Si), aluminum (Al), sodium (Na), and oxygen (O) element with the composition of 31.62, 9.04, 9.06, and 49.75, respectively. The presence of aluminum in silica gel reveals that this extraction process cannot remove aluminum very well. Therefore, silicon and oxygen show the highest composition, demonstrating the configuration of Si–O in the silica gel. Other than SiO_2, the
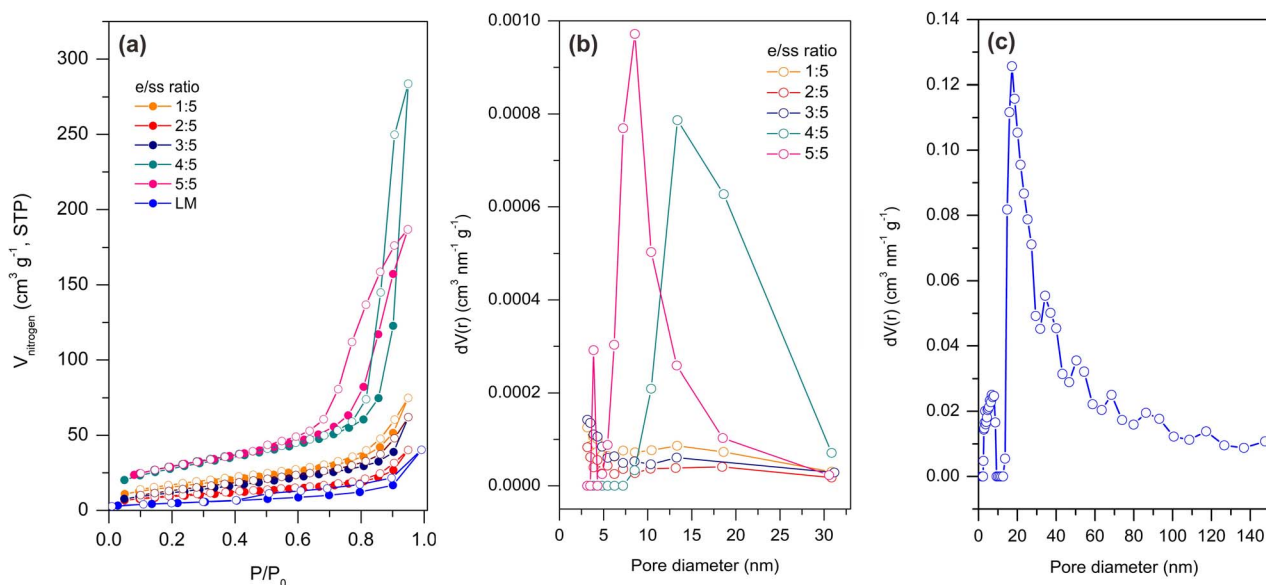

Fig. 3 Textural properties of silica gel. (a) N_2 adsorption–desorption behavior and pore size distribution of (b) silica gel and (c) LM.

Table 2 Textural properties of the synthesized silica gel

Textural properties	LM	e/ss ratio				
		1 : 5	2 : 5	3 : 5	4 : 5	5 : 5
Specific surface area^a (m^2 g^{-1})	17.3	57.2	33.2	45.6	100.1	103.5
Total pore volume^a (cm^3 g^{-1})	0.06	0.08	0.04	0.06	0.19	0.24
Average pore diameter^a (nm)	14.4	5.6	5.0	5.3	7.6	9.4
Mesopore surface area^b (m^2 g^{-1})	28.5	33.1	16.6	29.4	75.0	82.0
Mesopore volume^b (nm)	0.06	0.10	0.05	0.08	0.45	0.30
Mesopore diameter^b (nm)	17.2	3.2	3.2	3.2	13.4	8.5

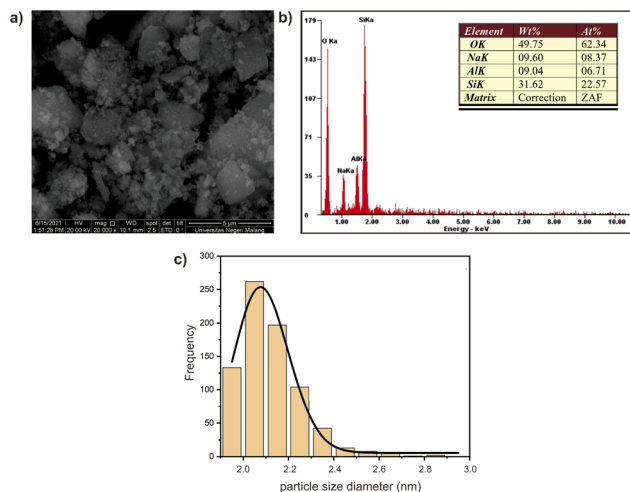^{a} Calculated by BET method. ^{b} Calculated by BJH desorption.

Fig. 4 (a) SEM images, (b) EDX, and (c) pore size distribution of silica gel (e/ss ratio of 5 : 5).

amount of O element in the obtained silica gel can be due to the configuration of Al_2O_3, Na_2O, $NaSiO_3$, or $NaAlO_2$.

Humidity test

As shown in Fig. 5, all silica gel takes up measurable quantities of water at different RH values of 70–90% at 29 ± 1 °C, which shows that the synthesized silica gel is a high-performance silica gel. The adsorption ability of silica gel (5 : 5) is the highest compared to that one, with the water adsorption value of 6.30% at RH of 70%, while the poor adsorption ability is showed by silica gel (1 : 5) with the water adsorption value of 1.8%. It can be connected to the number of active sites on the silica gel (5 : 5) being more abundant than silica gel (1 : 5), which is a crucial factor in the adsorption process.[30,31] Therefore, the adsorption performance at RH of 80% is more higher than that of 70% and 90%, explaining that the optimum adsorption process occurs with an RH of 80%. However, the trend of moisture adsorption by other silica gels showed a decrease capacity, indicating that the equilibrium of the adsorption–desorption state was reached due to surface adsorbent being saturated.

TGA analysis is also carried out at a temperature range of 28–600 °C to support the result. The determination of the adsorption capacity of the synthesized silica gel is based on the weight

loss during the TGA analysis. The weight loss is calculated at 100 °C, which indicates that the physically adsorbed water evaporation occurs at that temperature. As shown in Fig. 6, the TGA curve is a desorption/drying curve type, indicating that the weight loss in the samples is the mass of water. This data is supported by DTA results, which showed the presence of the first downward curve, indicating the heat adsorption process by samples at 100 °C as a dehydration event due to an endothermic reaction.[32] From that, the synthesized silica gel (5 : 5) shows the highest adsorption performance than others, indicating that the silica gel (5 : 5) has a high number of OH groups that can interact with water molecules *via* the hydrogen bridge.[33] This result is in agreement with the conventional gravimetric
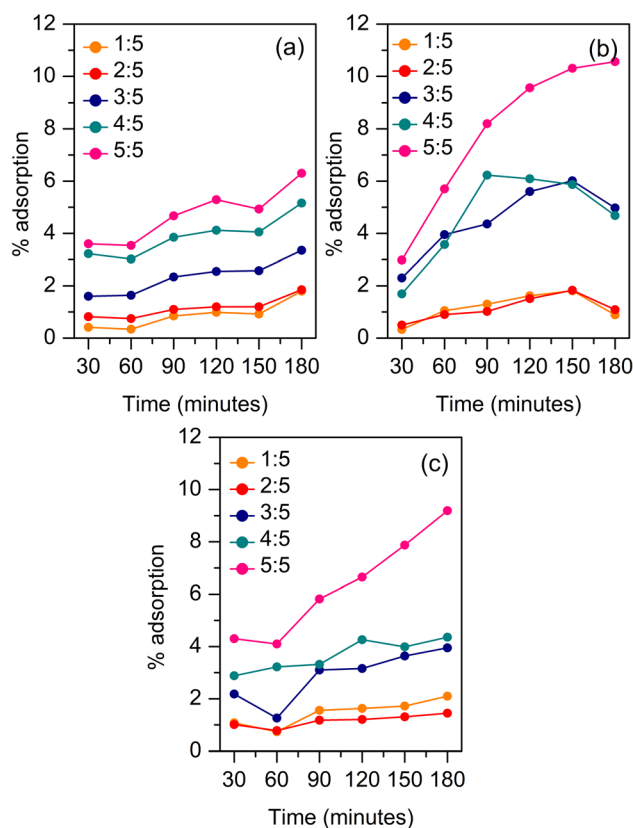

Fig. 5 Water adsorption by silica gel with humidity value of (a) 70%, (b) 80%, and (c) 90%.
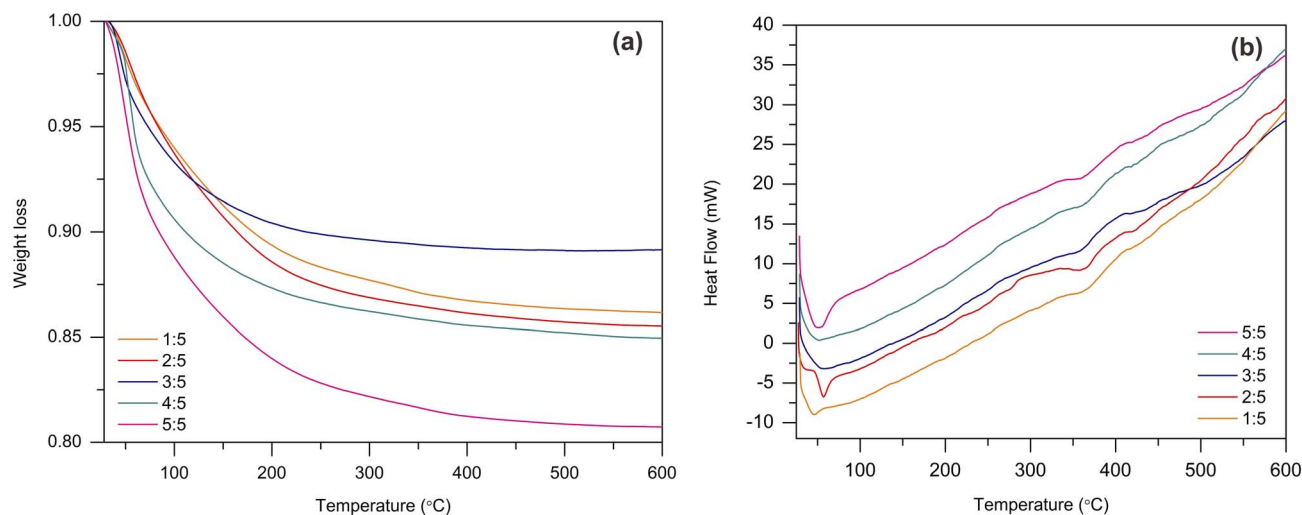
Fig. 6 TGA (a) and DTA (b) results of each silica gel after the adsorption process at 80% RH.

adsorption test. However, the adsorption ability of the silica gel (5 : 5) using TGA analysis is higher than that using the conventional gravimetric process, indicating that TGA analysis is suitable for the determination of adsorbed water molecule on silica gel.

Compared to commercial silica gel that has the highest adsorption capacity of the five investigated commercial silica gel samples, the 3 : 5, 4 : 5, and 5 : 5 silica gel exhibits higher adsorption ability than the commercial silica gel at RH value of 80%, both measured by the conventional gravimetric process and TGA analysis (see Fig. 7). The commercial silica gel exhibits the water adsorption performance of 1.8%. It can be inferred that the synthesized silica gel has a good adsorption capacity compared to commercial silica gel, indicating that the synthesized silica gel exhibits more active sites for adsorption. This result shows that the presence of ethanol gives an influence in the textural properties of silica gel, which is advantages for adsorption.

According to the results, the excellent adsorption performance is showed by the silica gel (5 : 5) in both conventional gravimetric measurement and using TGA analysis. Increasing the volume of ethanol can improve the active sites for the adsorption process, which is proven by the N_2 adsorption–desorption result. The high content of ethanol as a co-solvent promotes the polycondensation process rapidly and the formation of the alkoxide compound. The alkoxide compound will fill the pores of the gel, which is removed *via* heat treatment to form the pores in the silica gel. Increasing the amount of ethanol also enhances the layer porosity and pore diameter of the silica gel, causing the surface area to increase and more water to be adsorbed on the surface.[34]

According to the FTIR result, the silica gel (5 : 5) shows the highest silanol groups at 960 cm^{-1}, improving the

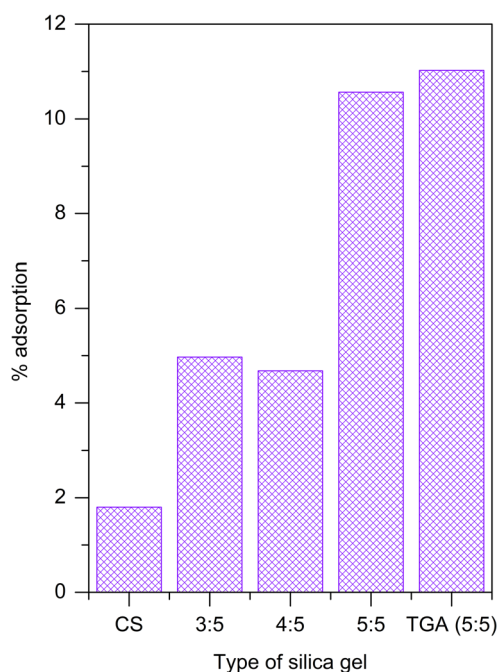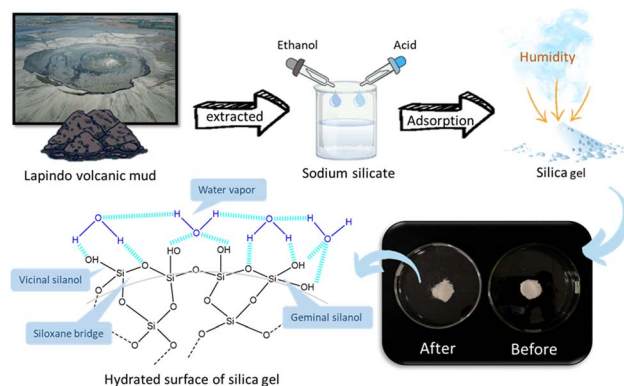**Fig. 7** Adsorption performance comparison of commercial and synthesized silica gel.

Fig. 8 Schematic illustration silica gel synthesis from Lapindo volcanic mud for desiccant application.

Table 3 Performance of silica gel in several reported papers

Materials	Surface area ($m^2 g^{-1}$)	Adsorption capacity ($g_{water} g_{adsorbent}^{-1}$)	Adsorption condition	Ref.
Silica gel	—	1.57	RH = 90%, T = 25 °C	37
Chitosan-SBA-15	106	1.37	RH = 90%, T = 25 °C	37
Chitosan/boehmite	—	1.5	RH = 60 ± 5%, T = 30 ± 2 °C	38
Alginate/silica gel	106.2	0.25	RH = 70%, T = 20 °C	39
Silica gel	347	0.19	RH = 70%, T = 20 °C	39
Silica gel from bagasse ash	152	0.18	RH = 100%, T = 30 °C	34
Silica gel from LM	103.5	0.11	RH = 80%, T = 29 ± 1 °C	This study

hydrophilicity properties of the silica gel (5 : 5). Consequently, the adsorption of water vapor is enhanced by hydrogen bridge interaction between OH groups in silica with lone pair of electrons of oxygen and hydrogen in water and/or the lone pair electron in the silanol group of silica and hydrogen element in water.[35,36] The interaction between vicinal silanol, geminal silanol, and siloxane bridge on the silica gel surface with water vapor is shown in Fig. 8, which gives the hydrated surface of the silica gel. The physical appearance of silica gel is the transparent lumps of crystals and becomes slightly dull after hydration. The unique textural properties of the synthesized silica gel generate a higher adsorption performance compared to commercial silica gel.

Several reported articles have been summarized in Table 3 to compare the capability of the obtained silica gel. The obtained silica gel exhibited a lowest water adsorption capacity compared to others. The modification of silica gel in the reported articles influenced the silica gel performance. For instance, the presence of chitosan or alginate on silica gel enhanced the water adsorption capability.[37–39] In conclusion, the modification of the obtained silica gel can be carried out to improve its performance.

Conclusion

Converting LM into silica gel was done by hydrometallurgy methods, followed by sol–gel methods for water vapor adsorption. The influence of the co-solvent, *i.e.*, ethanol, was carried out, exhibiting different textural properties. Increasing the amount of ethanol in the synthesis process enhances the number of hydroxyl groups in the silica gel structure, which is beneficial for water vapor adsorption. In addition, increasing the amount of ethanol also improves the specific surface area and porosity, providing more active sites for adsorption. The adsorption of water using the conventional gravimetric process and TGA analysis showed that the synthesized silica gel has a good adsorption capacity compared to the commercial silica gel. The synthesized silica gel with an e/ss ratio of 5 : 5 generated the highest adsorption capacity than others, which is in agreement with the hydroxyl groups and the specific surface area of the synthesized silica gel (5 : 5).

Author contributions

Qurrota A'yuni: conceptualization, methodology, supervision, validation, writing – review & editing. Ardhana Rahmayanti:

data curation, formal analysis, investigation. Hartati: validation, supervision, methodology. Purkan: validation, supervision. Riki Subagyo: writing – original draft, data curation. Nihayatur Rohmah: writing – review & editing. Luthfiyah Rifdah Itsnaini: investigation, writing – original draft. Medya Ayunda Fitri: visualization, project administration.

Conflicts of interest

The authors have no competing interests.

Acknowledgements

Notes and references

1 A. S. Norazam, H. M. Kamar, N. Kamsah dan and M. I. Alhamid, *Int. J. Technol.*, 2019, **10**, 1120–1130.

2 M. Sahlot dan and S. B. Riffat, *Int. J. Low-Carbon Technol.*, 2016, **11**, 489–505.

3 D. Balköse, S. Ulutan, F. Ç. Özkan, S. Çelebi dan and S. Ülkü, *Appl. Surf. Sci.*, 1998, **134**, 39–46.

4 A. Rahmayanti, Q. A'yuni, H. Hartati, P. Purkan dan and I. G. Romanza, *IOP Conf. Series: Earth and Environmental Science*, 2020, **456**.

5 U. Zulfiqar, T. Subhani dan and S. Wilayat Husain, *J. Non. Cryst. Solids*, 2015, **429**, 61–69.

6 Y. Fan, Y. Yang, B. Niu, Z. Liu, J. Dan dan and J. Wang, *Waste Manag.*, 2021, **131**, 359–367.

7 A. A. Mohamed Ismail, K. Kannadasan, P. Pichaimani, H. Arumugam dan and A. Muthukaruppan, *J. Clean. Prod.*, 2020, **264**, 121689.

8 E. Kamseu, L. M. Beleuk à Moungam, M. Cannio, N. Billong, D. Chaysuwan, U. C. Melo dan and C. Leonelli, *J. Clean. Prod.*, 2017, **142**, 3050–3060.

9 H. Mcmichael, *Bull. Indones. Econ. Stud.*, 2015, **45**, 37–41.

10 N. B. Talib, S. Triwahyono, A. A. Jalil, C. R. Mamat, N. Salamun, N. A. A. Fatah, S. M. Sidik dan and L. P. Teh, *Energy Convers. Manag.*, 2016, **108**, 411–421.

11 A. Mazzini, G. Etiope dan and H. Svensen, *Earth Planet. Sci. Lett.*, 2012, **317–318**, 305–318.

12 W. Trisunaryanti, A. Alethiana, I. I. Falah dan and D. A. Fatmawati, *React. Kinet. Mech. Catal.*, 2022, **135**, 951–970.

13 U. Zulfiqar, T. Subhani dan and S. W. Husain, *J. Asian Ceram. Soc.*, 2016, **4**, 91–96.

14 U. Zulfiqar, T. Subhani dan and S. Wilayat Husain, *J. Sol-Gel Sci. Technol.*, 2016, **77**, 753–758.

15 P. Khodaee, N. Najmoddin dan and S. Shahrad, 2018 *25th Iran. Conf. Biomed. Eng. 2018 3rd Int. Iran. Conf. Biomed. Eng. ICBME 2018*, 2018, 1–5.

16 D. Valeev, D. Pankratov, A. Shoppert, A. Sokolov, A. Kasikov, A. Mikhailova, C. Salazar-concha dan and I. Rodionov, *Trans. Nonferrous Met. Soc. China*, 2021, **31**, 3128–3149.

17 S. an Zheng, X. Zheng dan and C. Chen, *PLoS One*, 2012, 7, 1–7.

18 I. F. Ulfindrayani, N. Fanani, Q. A'yuni, N. Ikhlas, B. L. Gaol dan and D. Lestari, in *e-Prosiding SNasTekS*, 2019, hal. 235–240.

19 F. Mohamed, M. Shaban, G. Aljohani dan and A. M. Ahmed, *J. Mater. Res. Technol.*, 2021, **14**, 3140–3149.

20 A. Lesbani, P. Tamba and R. Mohadi dan Fahmariyanti, *Indones. J. Chem.*, 2013, **13**, 176–180.

21 A. Roy, *Colloids Surfaces A Physicochem. Eng. Asp.*, 2021, **608**, 125574.

22 M. A. Bhosale, D. Ummineni, T. Sasaki, D. Nishio-Hamane dan and B. M. Bhanage, *J. Mol. Catal. A Chem.*, 2015, **404–405**, 8–17.

23 P. Velmurugan, J. Shim, K. J. Lee, M. Cho, S. S. Lim, S. K. Seo, K. M. Cho, K. S. Bang dan and B. T. Oh, *J. Ind. Eng. Chem.*, 2015, **29**, 298–303.

24 T. J. Siang, A. A. Jalil dan and M. Y. S. Hamid, *Mater. Today Chem.*, 2022, **23**, 100684.

25 H. Tehubijuluw, R. Subagyo, M. F. Yulita, R. E. Nugraha, Y. Kusumawati, H. Bahruji, A. A. Jalil, H. Hartati dan and D. Prasetyoko, *Environ. Sci. Pollut. Res.*, 2021, **28**, 37354–37370.

26 A. F. A. Rahman, A. A. Jalil, M. Y. S. Hamid, I. Hussain, N. S. Hassan dan and A. H. Khoja, *Mol. Catal.*, 2022, **526**, 112370.

27 A. A. Widati, M. Z. Fahmi, S. C. W. Sakti, T. A. Budiastanti dan and T. E. Purbaningtias, *J. Manuf. Mater. Process.*, 2022, **6**, 101.

28 R. E. Nugraha, D. Prasetyoko, H. Bahruji, S. Suprapto, N. Asikin-Mijan, T. P. Oetami, A. A. Jalil, D. V. N. Vo dan and Y. H. Taufiq-Yap, *RSC Adv.*, 2021, **11**, 21885–21896.

29 R. M. M. Santos, J. Tronto, V. Briois dan and C. V Santilli, *J. Mater. Chem. A*, 2017, **5**, 9998–10009.

30 C. Qi, L. Xu, M. Zhang dan and M. Zhang, *Microporous Mesoporous Mater.*, 2019, **290**, 109651.

31 H. Li, V. L. Budarin, J. H. Clark, M. North dan and X. Wu, *J. Hazard. Mater.*, 2022, **436**, 129174.

32 R. S. Mustopa dan and D. D. Risanti, *J. Tek. Pomits*, 2013, **2**, 1–6.

33 Y. Han, Z. Yan, L. Jin, J. Liao dan and G. Feng, *RSC Adv.*, 2020, **10**, 16949–16958.

34 S. Affandi, H. Setyawan, S. Winardi, A. Purwanto dan and R. Balgis, *Adv. Powder Technol.*, 2009, **20**, 468–472.

35 P. Kumar, S. Kumar, A. Kumar dan and V. Verma, *J. Mater. Sci. Mater. Electron.*, 2021, **32**, 14833–14845.

36 V. G. Plotnichenko, V. O. Sokolov dan and E. M. Dianov, *Inorg. Mater.*, 2000, **36**, 404–410.

37 M. Ignat, P. Samoila, C. Cojocaru, G. Soreanu, I. Cretescu dan and V. Harabagiu, *Appl. Surf. Sci.*, 2019, **487**, 1189–1197.

38 M. Rajamani dan and S. M. Maliyekkal, *Carbohydr. Polym.*, 2018, **194**, 245–251.

39 X. Zheng, K. Chen dan and Z. Lin, *Ind. Eng. Chem. Res.*, 2020, **59**, 5760–5767.